Critical metal enrichment in crustal melts: the role of metamorphic mica

Critical metal enrichment in crustal melts: the role of metamorphic mica

Barbara E. Kunz, Clare J. Warren, Frances E. Jenner, Nigel B.W. Harris, Tom W. Argles

School of Environment, Earth and Ecosystem Sciences, The Open University, Walton Hall, Milton Keynes, MK7 6AA, UK

Contact: barbara.kunz@open.ac.uk

ABSTRACT

Metals such as Li, Be, V, Co, Nb, In, Cs, Sn, Ta, and W are considered resources that are critical for modern economies. They can be significantly enriched in granites and pegmatites, but the mechanisms of enrichment remain poorly understood. Many metal-enriched granitic magmas form through mica dehydration reactions during high-grade metamorphism. The preferential incorporation of these metals into micas provides a mechanism for concentration and mobilisation during crustal melting. Comprehensive datasets of these elements and their partitioning in metamorphic micas across different metamorphic grades are currently lacking. We present the first extensive *in-situ* LA-ICP-MS element dataset collected from metasediment-hosted muscovite and biotite from three different metamorphic cross-sections traversing sub-greenschist (~400°C) to granulite-facies conditions (>900°C). Within the same sample, Li, V, Co, Cs, and Ta concentrations are higher in biotite, whereas Be, In, Sn, and W concentrations are higher in muscovite. Sub-solidus micas record only non-systematic compositional variations between samples. Supra-solidus biotites show systematic depletion in Li, Be, Sn and Cs and enrichment in V and Co with increasing temperature in the highest-grade (muscovite-absent) samples. Indium and W reach peak concentrations in biotite at 750°C and 850°C respectively. Muscovites record systematic enrichment in In and W and

depletion in Be, Sn and Cs with increasing metamorphic grade. These distinctive trends appear independent of tectonic setting (i.e. continental collision and crustal thinning). Our dataset highlights the importance of higher-temperature melting (>750°C), in particular, biotite breakdown reactions, for the release of Li, Be, Sn, Cs and W into crustal melts.

INTRODUCTION

Most trace metal-enriched granites and pegmatites (e.g. Li-Cs-Ta) are highly peraluminous, suggesting they formed via mica-melting reactions from metasedimentary protoliths (e.g., Patiño Douce and Harris, 1998; Cerny et al., 2012). During these reactions, trace elements that are hosted in micas may be released into the melt (Dahl et al., 1993). Along with enriched protolith compositions (Clemens et al., 2009; Romer and Kroner 2016; Wolf et al., 2018), melting reactions may play an important role in generating crustal magmas that are sufficiently enriched to eventually fuel formation of critical metal deposits at shallower levels in the crust (e.g., Linnen et al., 2012; London, 2018). Both fluid-present and fluid-absent reactions involving micas will generate melt, with muscovite melting at lower temperatures and biotite melting at higher temperatures (e.g., Weinberg and Hasalová, 2016).

The concentrations of different elements in these micas, and their behaviour during melting reactions, will influence the composition of the melt produced at different temperatures (Wolf et al., 2018). For example, residuum (melanosomes) in migmatites that formed by muscovite-melting reactions at ~750°C in the Iberian Massif (Spain) are enriched in metals such as Li, Cs, Sn and W compared to the crystallised partial melt (leucosome). However both leucosomes and melanosomes in slightly higher temperature (800°C) migmatites generated by biotite-melting reactions record similar concentrations of these elements (Wolf et al., 2018). These data suggested that higher temperature melting reactions release critical metals (previously stored in restitic mineral phases) into the melt.

It is unclear if these trends and observations can be applied more generally to crustal melting over a larger range of temperatures, different tectonic settings and different protolith compositions. Additionally, direct comparisons between the compositions of leucosomes and melanosomes are compromised by magmatic dilution, crystallisation, segregation or transport (Wolf et al., 2018). The role of sub- and supra-solidus metamorphic reactions in concentrating and releasing critical elements is also poorly constrained. These shortcomings make it difficult to assess why granites that are generated by crustal melting have such variable critical element concentrations. Here we present a new approach for placing constraints on the partitioning of critical elements with increasing temperatures during crustal melting. By measuring the concentrations of 57 elements *in-situ* in muscovite and biotite from metapelites at different metamorphic grades, we have found systematic changes in the concentrations of different critical metals as temperatures rise and dehydration reactions initiate. This provides a new opportunity to constrain the input of different critical metals into crustal melts at different stages of the metamorphic-melting cycle.

METHODS and SAMPLE MATERIAL

We analysed trace element concentrations by LA-ICP-MS in muscovite and biotite in 22 samples from three different metamorphic cross-sections covering sub-greenschist to granulite-facies conditions. Supplementary material S1–4 contains sample descriptions, mineral assemblages, analytical methods and photomicrographs showing laser spot locations. The full dataset of major and trace elements, secondary standards and all element plots are presented in Table S5.

We selected samples from two different tectonic settings. The samples from the Himalayas were metamorphosed during continent-continent collision, whereas the samples

from the Ivrea Zone received their metamorphic imprint during post-orogenic collapse and extension.

The eight samples labelled SK-10-XX were collected from a cross-section through the 5–10 km-thick Main Central Thrust in the Sikkim Himalaya, India. An inverted prograde metamorphic sequence is well-developed across this ductile structure, from low-greenschist (chlorite and biotite grades) at the lowest levels through to upper-amphibolite (kyanite and sillimanite grade) at the highest levels. The sampling localities, sample descriptions and pressure-temperature results are documented in detail in Mottram et al. (2014). This sample set covers the onset of muscovite melting.

The four samples labelled N-XX were collected from the hanging wall of the Main Central Thrust in the Langtang Himalaya, Nepal, from higher structural levels and similar metamorphic grades to the highest-grade Sikkim samples. These samples were metamorphosed at kyanite to sillimanite grade, with coarser leucocratic streaks and patches interpreted as leucosome in samples N5 and N11, across the muscovite-out isograd.

The ten IZ-4XX samples were collected from the Val Strona di Omega, in the Ivrea Zone of the European Alps, Italy. They were metamorphosed at upper amphibolite to granulite facies conditions, and show both muscovite and biotite melting reactions. Sampling localities, sample descriptions and pressure-temperature results are documented in detail in Kunz et al. (2018) and Kunz and White (2019).

RESULTS

The within-sample average concentrations of 26 elements in biotite and muscovite shown in Fig. 1 are normalised to Bulk Silicate Earth concentrations (Palme and O'Neill, 2013) and plotted in order of increasing bulk partitioning behaviour (Jenner, 2017). Both biotite and muscovite record concentration variability within and between samples, and

record enrichments and depletions in the concentrations of some critical elements (e.g., Sn, In, Cs) compared to the composition of the bulk continental crust. We have not observed any systematic patterns in element concentrations with petrographic location. The lowest-temperature samples SK12 and SK15 were too fine grained to acquire "clean" analyses of individual micas and the data are not presented.

Elemental concentrations in biotite vary more systematically than in muscovite particularly in the high-temperature samples from the Ivrea Zone compared to the samples from the lower grade Sikkim section (Figs. 2 and 3; Tab. S1). Specifically, there are systematic changes of up to two orders-of-magnitude in the concentrations of Li, Be, F, V, Co, Nb, In, Sn, Cs, Ta, and W with increasing metamorphic grade that are all greater than analytical uncertainty; we have therefore focussed attention on these eleven elements. Additionally, there are clear differences in concentration between the different field areas that are most likely related to different bulk rock abundances of these elements.

Typically, biotite contains higher concentrations of Li, F, V, Co, Nb, Cs and Ta than muscovite, whereas muscovite systematically hosts higher concentrations of Be, In, Sn and W (Figs. 2 and 3). Concentrations of most elements in muscovite generally show little to no systematic change with increasing metamorphic temperature except in the Langtang samples which show increases in In and W concentrations and decreases in Li, Be and Cs concentrations at supra-solidus temperatures.

Sub-solidus biotites in the Sikkim samples show no systematic changes in trace element concentration. Above solidus temperatures, biotite in the Langtang and Ivrea Zone samples show a gradual decrease in Li, Cs, Be and Sn concentrations and an increase in V and Co concentrations with increasing temperature (Fig. 2). Concentrations of In and W increase in biotite as temperatures increase to ~850 and 750°C respectively; concentrations then decrease with increasing metamorphic grade (Fig. 2). Ta and Nb concentrations remain

fairly constant in biotite with increasing metamorphic temperature, except in the two highest-grade samples that have abundant rutile (Fig. 3).

DISCUSSION

Controls on trace element concentrations in sub-and supra-solidus phases

Our data show that Li, Cs and Ta (commonly enriched together in LCT-pegmatites) are predominantly hosted in biotite, while Be, Sn and W are predominantly hosted in muscovite (c.f. Dutrow et al., 1986; Dahl et al., 1993; Bea et al., 1994; Yang and Rivers, 2000; Tischendorf et al., 2001; Neiva et al., 2002; Van Lichtervelde et al., 2008; Simons et al., 2017). In the sub-solidus samples, concentrations of most critical metals measured in both micas are variable and show no systematic changes. For example in the Sikkim samples SK19–SK22 (which equilibrated at similar temperatures within uncertainty of 650–700°C) we observe an order-of-magnitude difference in Li and Ta concentrations in both micas. We therefore interpret this as either reflecting (i) differences in bulk composition and therefore different initial trace element abundance (Romer and Kroner, 2016), or (ii) differences in the continuity of this metamorphic sequence due to ductile deformation.

Partitioning of metals between biotite and muscovite can be explained by differences in site and interlayer site preferences of these elements (Dahl et al., 1993). The apparent increase in concentration of V, Co and In in biotite with increasing metamorphic grade could be an effect of decreasing modal abundance of biotite. However, the concentration increase starts at the onset of muscovite melting when the modal abundance of biotite is still increasing. Therefore we interpret the observed trends for these elements as resulting from differential partitioning in the presence of a melt phase. Conversely, the increase of W in muscovite coincides with the decrease in modal abundance of muscovite, suggesting that this might be a modal abundance effect.

The partitioning of critical metals between micas and other metamorphic minerals may also be important at sub- and supra-solidus conditions. For example Li is hosted in tourmaline and staurolite (e.g., Dutrow et al., 1986; London, 2011), Be in cordierite (Evensen and London, 2002) and Sn and W in rutile, ilmenite and titanite (e.g., Zack et al., 2002; Klemme et al., 2006). However, there are currently only sparse datasets for many critical metals for solid/solid partitioning at high-temperature metamorphic conditions (e.g., Icenhower and London, 1995; Dutrow et al., 1986) making a quantification of partitioning difficult to assess.

Implications for the formation of enriched granites and pegmatites

Our dataset demonstrates the importance of melting reactions involving biotite for the concentration (in the melanosome) and release (into the leucosome) of a number of critical metals, specifically Li, Be, Sn, Cs and W. Biotite is widely present in a variety of bulk-rock compositions and is a known host of critical metals (e.g. Dahl et al., 1993; Evensen and London, 2002). Our data show that concentrations of these elements in metapelitic biotite remains approximately constant until the onset of biotite dehydration melting reactions, when these elements are released into the melt. Our findings are in agreement with bulk rock data from the Ivrea Zone (Bea and Montero, 1999) that show a similar depletion in bulk rock for Li, Be, Cs and an increase in V with metamorphic grade.

This scenario of high-temperature biotite melting as the key for the enrichment of Li-Cs-Ta in the melt is in conflict with previous hypothesis of LCT-enriched pegmatites being generated by minimum-temperature melting of muscovite (e.g. Cerny, 1991; Romer and Kroner, 2015, 2016). Instead, our data suggest that enrichment of LCT-enriched granitic magmas most likely occurs during low-volume biotite melting of a mostly muscovite-absent assemblage, a scenario that has also been argued for granitic Sn enrichment (Wolf et al.,

174 2018) and the enrichment patterns of successive granite suites of the Cornubian Batholith in
175 Cornwall, UK (Simons et al., 2017).

176 Biotite provides the source of these elements as well as a mechanism for allowing
177 more effective melt and metal transport. Crustal melts are viscous (Rutter and Neumann,
178 1995) and therefore difficult to mobilise without additional help, e.g. from pervasive ductile
179 deformation or the addition of fluxing elements such as F, which lower melt viscosity
180 (Dingwell et al., 1996). Additionally, F allows metals to be transported in the melt more
181 readily through complexing (London, 1987). High-temperature biotite can host F at weight-%
182 levels (Finch and Tomkins, 2016); in our samples the Sikkim and Ivrea Zone biotites contain
183 higher F concentrations than muscovite (0.13–1.6 wt% F compared to 0.04–0.16 wt% F
184 respectively; Fig 2).

185 Sn and W enrichments in granites have been linked to high-temperature melting of a
186 biotite-rich source (Romer and Kroner, 2016; Wolf et al., 2018). Our data show that, in
187 general, concentrations of Sn and W are higher in muscovite than in co-hosted biotite.
188 Concentrations of W in muscovite increase slightly with metamorphic grade; we do not
189 observe systematic changes of Sn concentrations in muscovite with metamorphic grade. In
190 contrast, biotite from the Ivrea Zone and Langtang samples show clear decreases in Sn and W
191 concentrations with increasing metamorphic grade. This observation supports the theory of
192 higher-temperature melting being critical for melt enrichment (Wolf et al., 2018; Michaud et
193 al., 2021). However we do not observe sequestering of Sn into biotite across the muscovite-
194 melting temperature interval, as previously suggested (Wolf et al., 2018).

195 Further investigation into different biotite melting reactions, including those which
196 are fluid-absent or fluid-present, are needed to understand the conditions/reactions under
197 which critical metal release is optimised and therefore provides the highest potential for melt
198 enrichment. Biotite is also a key constituent in non-pelitic metasesediments (e.g. meta-

199 graywackes) that may also be source rocks for enriched granites and pegmatites. Focus on
200 biotite-melting reactions across a range of metasedimentary bulk compositions is therefore
201 key to constraining how and under which conditions critical metal enriched granites and
202 pegmatites form.
203
204 **CONCLUSIONS**
205 Micas are the main reactant during dehydration melting of metasediments. As micas host
206 significant concentrations of many critical metals and H_2O, their breakdown facilitates the
207 transfer of these metals from metamorphosed country rocks into melts. Our data show that
208 prograde sub-solidus metamorphic reactions do not lead to systematic changes in the
209 concentrations of different critical metals in micas. Upon crossing the muscovite dehydration
210 solidus, both muscovite and biotite concentration for Cs and Be start to decrease, while W
211 concentration increase. Once conditions for biotite dehydration melting are reached,
212 concentrations of Li, Be, Sn, Cs, and W in biotite decrease markedly as they are released into
213 the melt.
214
215 **ACKNOWLEDGMENTS**
216 We'd like to thank G. Degli-Alessandrini for help with EMPA work at the OU. K.
217 Goodenough and R. Shaw (BGS) for fruitful discussions and C. Mottram for providing thin
218 sections from the Sikkim section. We thank three anonymous reviewers for their constructive
219 comments and Gerald Dickens for editorial handling.
220
221 **FIGURE CAPTIONS**
222 **Fig. 1** Average trace element concentration per sample of (a) muscovite (b) biotite.
223 Normalised to Bulk Silicate Earth (Palme and O'Neill, 2013); black line is the composition of

the bulk continental crust (Rudnick and Gao, 2003); element ordering is based on bulk partitioning during differentiation of mid-ocean ridge basalts (Jenner, 2017).

Fig. 2 Concentrations of Li, F, Cs, Be, Sn, W, V, Co and In *vs.* peak metamorphic temperature. Grey shaded areas represent muscovite- (light grey) and biotite-melting (dark grey) ranges. Trends in: biotite (solid arrow), muscovite (dashed arrow) data.

Fig. 3 Concentration of Nb and Ta *vs.* peak metamorphic temperature. Grey shaded areas represent muscovite- (light grey) and biotite-melting (dark grey) ranges. Trends in: biotite (solid arrow), muscovite (dashed arrow) data.

SUPPLEMANTARY MATERIAL

APPENDIX 1. Sample description

APPENDIX 2. Table with mineral assemblages

APPENDIX 3. Detailed method description for LA-ICP-MS analysis

APPENDIX 4. LA-ICP-MS spot location

APPENDIX 5. Major and trace element data table for samples and secondary standard

REFERENCES CITED

Bea, F., and Montero, P., 1999, Behavior of accessory phases and redistribution of Zr , REE , Y , Th , and U during metamorphism and partial melting of metapelites in the lower crust : An example from the Kinzigite Formation of Ivrea-Verbano , NW Italy: Geochimica et Cosmochimica Acta, v. 63, p. 1133–1153.

Bea, F., Pereira, M.D., and Stroh, A., 1994, Mineral/leucosome trace-element partitioning in a peraluminous migmatite (a laser ablation-ICP-MS study): Chemical Geology, v. 117, p. 291–312, doi:10.1016/0009-2541(94)90133-3.

Černý, P., 1991, Fertile granites of Precambrian rare-element pegmatite fields: is geochemistry controlled by tectonic setting or source lithologies? Precambrian Research, v. 51, p. 429–468, doi:10.1016/0301-9268(91)90111-M.

Cerny, P., London, D., and Novak, M., 2012, Granitic Pegmatites as Reflections of Their Sources: Elements, v. 8, p. 289–294, doi:10.2113/gselements.8.4.289.

253 Clemens, J.D., Helps, P.A., and Stevens, G., 2009, Chemical structure in granitic magmas - A
254 signal from the source?, *in* Earth and Environmental Science Transactions of the Royal
255 Society of Edinburgh, Royal Society of Edinburgh Scotland Foundation, v. 100, p. 159–
256 172, doi:10.1017/S1755691009016053.

257 Dahl, P.S., Wehn, D.C., and Feldmann, S.G., 1993, The systematics of trace-element
258 partitioning between coexisting muscovite and biotite in metamorphic rocks from the
259 Black Hills, South Dakota, USA: Geochimica et Cosmochimica Acta, v. 57, p. 2487–
260 2505.

261 Dingwell, D.B., Romano, · C, and Hess, K.-U., 1996, The effect of water on the viscosity of a
262 haplogranitic melt under P-T-X conditions relevant to silicic volcanism: Contrib Mineral
263 Petrol, v. 124, p. 19–28.

264 Dutrow, B.L., Holdaway, M.J., and Hinton, R.W., 1986, Lithium in staurolite and its
265 petrologic significance: Contributions to Mineralogy and Petrology 1986 94:4, v. 94, p.
266 496–506, doi:10.1007/BF00376341.

267 Icenhower, J., and London, D., 1995, An experimental study of element partitioning among
268 biotite, muscovite, and coexisting peraluminous silicic melt at 200 MPa (H2O):
269 American Mineralogist, v. 80, p. 1229–1251, doi:10.2138/am-1995-11-1213.

270 Evensen, J.M., and London, D., 2002, Experimental silicate mineral/melt partition
271 coefficients for beryllium and the crustal Be cycle from migmatite to pegmatite:
272 Geochimica et Cosmochimica Acta, v. 66, p. 2239–2265, doi:10.1016/S0016-
273 7037(02)00889-X.

274 Finch, E.G., and Tomkins, A.G., 2017, Fluorine and chlorine behaviour during progressive
275 dehydration melting: Consequences for granite geochemistry and metallogeny: Journal
276 of Metamorphic Geology, v. 35, p. 739–757, doi:10.1111/jmg.12253.

277 Jenner, F.E., 2017, Cumulate causes for the low contents of sulfide-loving elements in the
278 continental crust: Nature Geoscience 2017 10:7, v. 10, p. 524–529,
279 doi:10.1038/ngeo2965.

280 Klemme, S., Günther, D., Hametner, K., Prowatke, S., and Zack, T., 2006, The partitioning of
281 trace elements between ilmenite, ulvospinel, armalcolite and silicate melts with
282 implications for the early differentiation of the moon: Chemical Geology, v. 234, p.
283 251–263, doi:10.1016/J.CHEMGEO.2006.05.005.

284 Kunz, B.E., Regis, D., and Engi, M., 2018, Zircon ages in granulite facies rocks: decoupling
285 from geochemistry above 850 °C? Contributions to Mineralogy and Petrology 2018
286 173:3, v. 173, p. 1–21, doi:10.1007/S00410-018-1454-5.

287 Kunz, B.E., and White, R.W., 2019, Phase equilibrium modelling of the amphibolite to
288 granulite facies transition in metabasic rocks (Ivrea Zone, NW Italy): Journal of
289 Metamorphic Geology, v. 37, p. 935–950, doi:10.1111/JMG.12478.

290 Linnen, R.L., Van Lichtervelde, M., and Cerny, P., 2012, Granitic Pegmatites as Sources of
291 Strategic Metals: Elements, v. 8, p. 275–280, doi:10.2113/gselements.8.4.275.

London, D., 1987, Internal differentiation of rare-element pegmatites: Effects of boron, phosphorus, and fluorine: Geochimica et Cosmochimica Acta, v. 51, p. 403–420, doi:10.1016/0016-7037(87)90058-5.

London, D., 2011, Experimental synthesis and stability of tourmaline: a historical overview: The Canadian Mineralogist, v. 49, p. 117–136, doi:10.3749/CANMIN.49.1.117.

London, D., 2018, Ore-forming processes within granitic pegmatites: Ore Geology Reviews, v. 101, p. 349–383, doi:10.1016/j.oregeorev.2018.04.020.

Michaud, J.A.-S., Pichavant, M., and Villaros, A., 2021, Rare elements enrichment in crustal peraluminous magmas: insights from partial melting experiments: Contributions to Mineralogy and Petrology, v. 176, p. 96, doi:10.1007/s00410-021-01855-9.

Mottram, C.M., Warren, C.J., Regis, D., Roberts, N.M.W., Harris, N.B.W., Argles, T.W., and Parrish, R.R., 2014, Developing an inverted Barrovian sequence; insights from monazite petrochronology: Earth and Planetary Science Letters, v. 403, p. 418–431, doi:10.1016/J.EPSL.2014.07.006.

Neiva, A.M.R., Silva, M.M.V.G., Gomes, M.E.P., and Campos, T.F.C., 2002, Geochemistry of coexisting biotite and muscovite of Portuguese peraluminous granitic differentiation series: Chemie der Erde, v. 62, p. 197–215, doi:10.1078/0009-2819-00007.

Palme, H., and O'Neill, H., 2013, Cosmochemical Estimates of Mantle Composition, *in* Treatise on Geochemistry: Second Edition, v. 3, p. 1–39, doi:10.1016/B978-0-08-095975-7.00201-1.

Patiño Douce, A.E., and Harris, N., 1998, Experimental constraints on Himalayan anatexis: Journal of Petrology, v. 39, p. 689–710, doi:10.1093/petroj/39.4.689.

Romer, R.L., and Kroner, U., 2015, Sediment and weathering control on the distribution of Paleozoic magmatic tin–tungsten mineralization: Mineralium Deposita, v. 50, p. 327–338, doi:10.1007/s00126-014-0540-5.

Romer, R.L., and Kroner, U., 2016, Phanerozoic tin and tungsten mineralization-Tectonic controls on the distribution of enriched protoliths and heat sources for crustal melting: Gondwana Research, v. 31, p. 60–95: doi:10.1016/j.gr.2015.11.002.

Rudnick, R.L., and S. Gao., 2003, Composition of the continental crust, *in* Holland H.D., and Turekian, K.K, *eds.*, Treatise on Geochemistry, v. 3-9, 1–64, doi:10.1016/B0-08-043751-6/03016-4.

Rutter, E.H., and Neumann, D.H.K., 1995, Experimental deformation of partially molten Westerly granite under fluid-absent conditions, with implications for the extraction of granitic magmas: Journal of Geophysical Research: Solid Earth, v. 100, p. 15697–15715, doi:10.1029/94JB03388.

Simons, B., Andersen, J.C.Ø., Shail, R.K., and Jenner, F.E., 2017, Fractionation of Li, Be, Ga, Nb, Ta, In, Sn, Sb, W and Bi in the peraluminousEarly Permian Variscan granites of

the Cornubian Batholith: Precursorprocesses to magmatic-hydrothermal mineralisation: Lithos, v. 278–281, p. 491–512, doi:10.1016/j.lithos.2017.02.007.

Tischendorf, G., Förster, H.-J., and Gottesmann, B., 2001, Minor- and trace-element composition of trioctahedral micas: a review: Mineralogical Magazine, v. 65, p. 249–276, doi:10.1180/002646101550244.

Van Lichtervelde, M., Grégoire, M., Linnen, R.L., Béziat, D., and Salvi, S., 2008, Trace element geochemistry by laser ablation ICP-MS of micas associated with Ta mineralization in the Tanco pegmatite, Manitoba, Canada: Contributions to Mineralogy and Petrology, v. 155, p. 791–806, doi:10.1007/s00410-007-0271-z.

Weinberg, R.F., and Hasalová, P., 2015, Water-fluxed melting of the continental crust: A review: Lithos, v. 212–215, p. 158–188, doi:10.1016/j.lithos.2014.08.021.

Wolf, M., Romer, R.L., Franz, L., and López-Moro, F.J., 2018, Tin in granitic melts: The role of melting temperature and protolith composition: Lithos, v. 310–311, p. 20–30, doi:10.1016/j.lithos.2018.04.004.

Yang, P., and Rivers, T., 2000, Trace element partitioning between coexisting biotite and muscovite from metamorphic rocks, Western Labrador: Structural, compositional and thermal controls: Geochimica et Cosmochimica Acta, v. 64, p. 1451–1472, doi:10.1016/S0016-7037(99)00425-1.

Zack, T., Kronz, A., Foley, S., and Rivers, T., 2002, Trace element abundances in rutiles from eclogites and associated garnet mica schists: Chemical Geology, v. 184, p. 97–122, doi:10.1016/S0009-2541(01)00357-6.

Figure 1

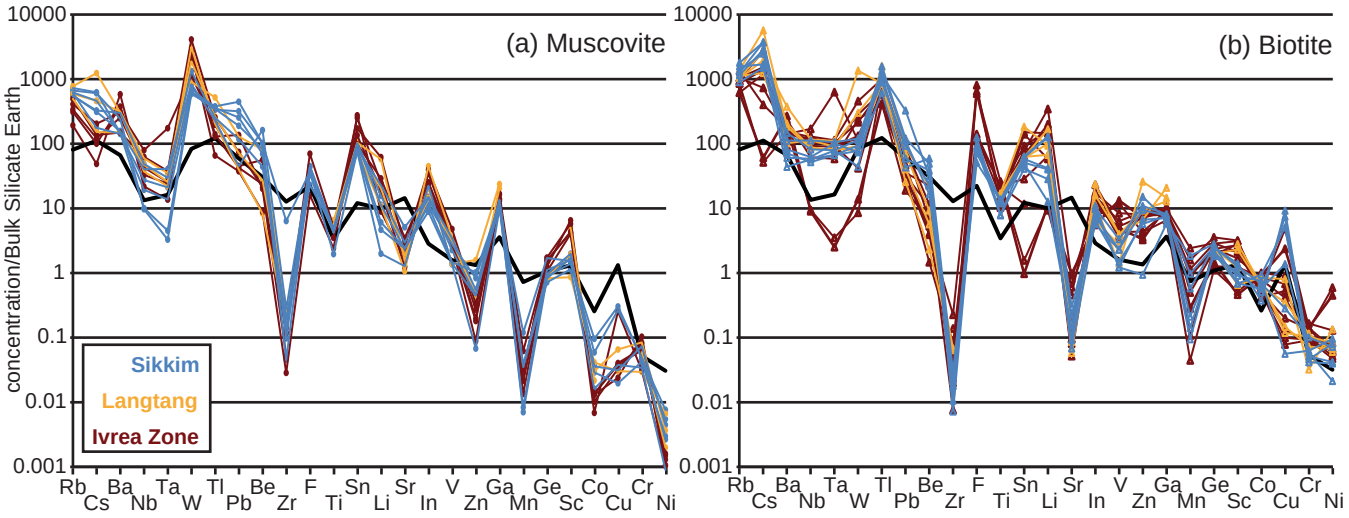

Kunz et al., Fig. 1

Figure 2

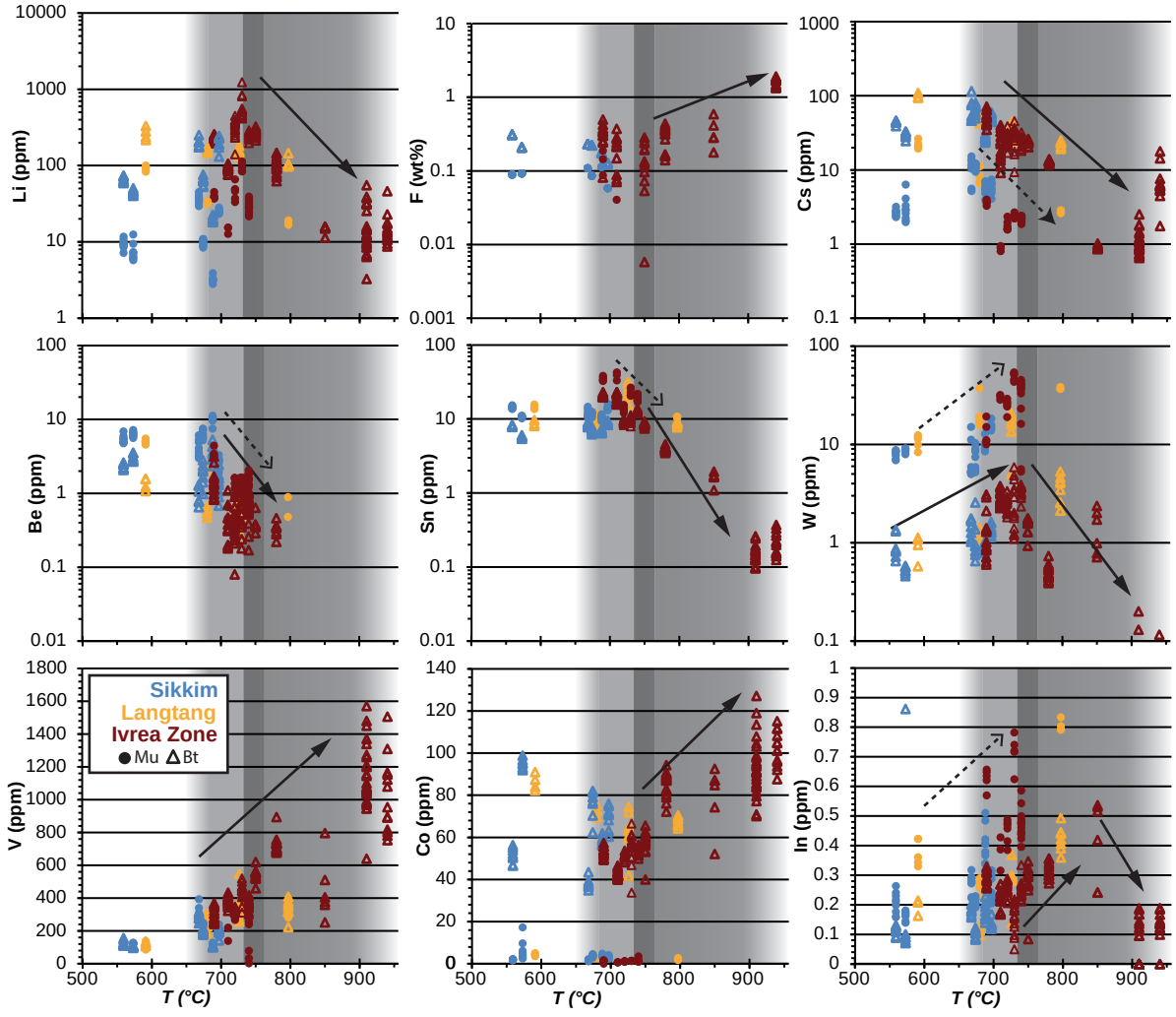

Kunz et al., Figure 2

Figure 3

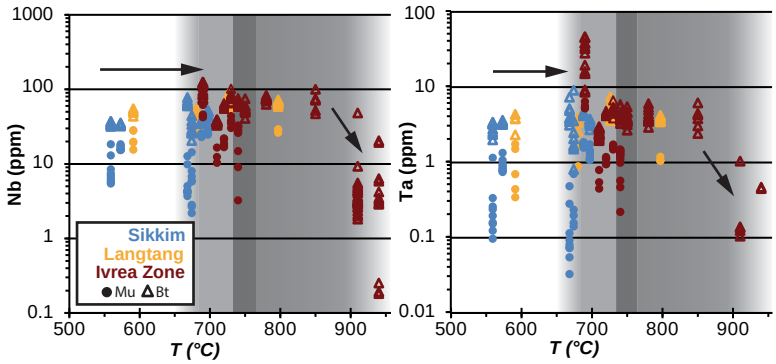

Kunz et al., Figure 3